Journal of Molecular and Cellular Cardiology 115 (2018) 39–50

Contents lists available at ScienceDirect

Journal of Molecular and Cellular Cardiology

journal homepage: www.elsevier.com/locate/yjmcc

Original article

ErbB2 promotes endothelial phenotype of human left ventricular epicardial highly proliferative cells (eHiPC)

Sergey Ryzhov[a], Michael P. Robich[a,b], Daniel J. Roberts[a,b], Amanda J. Favreau-Lessard[a], Sarah M. Peterson[a], Edward Jachimowicz[a], Rutwik Rath[a], Calvin P.H. Vary[a], Reed Quinn[b], Robert S. Kramer[b], Douglas B. Sawyer[a,b,*]

[a] Maine Medical Center Research Institute, Scarborough, ME, United States
[b] Maine Medical Center, Portland, ME, United States

ARTICLE INFO

Keywords:
Myocardium
Neuregulin
Cell biology
Cell differentiation

ABSTRACT

The adult human heart contains a subpopulation of highly proliferative cells. The role of ErbB receptors in these cells has not been studied. From human left ventricular (LV) epicardial biopsies, we isolated highly proliferative cells (eHiPC) to characterize the cell surface expression and function of ErbB receptors in the regulation of cell proliferation and phenotype. We found that human LV eHiPC express all four ErbB receptor subtypes. However, the expression of ErbB receptors varied widely among eHiPC isolated from different subjects. eHiPC with higher cell surface expression of ErbB2 reproduced the phenotype of endothelial cells and were characterized by endothelial cell-like functional properties. We also found that EGF/ErbB1 induces VEGFR2 expression, while ligands for both ErbB1 and ErbB3/4 induce expression of Tie2. The number of $CD31^{pos}CD45^{neg}$ endothelial cells is higher in LV biopsies from subjects with high ErbB2 ($ErbB2^{high}$) eHiPC compared to low ErbB2 ($ErbB2^{low}$) eHiPC. These findings have important implications for potential strategies to increase the efficacy of cell-based revascularization of the injured heart, through promotion of an endothelial phenotype in cardiac highly proliferative cells.

1. Introduction

Myocardial response to injury induces a proliferative response that is associated with intense angiogenesis [13,51,62] and cardiac repair, as well as adverse remodeling and development of heart failure [12,26]. Different subpopulations of cardiac cells, including fibroblasts [64], endothelial cells (EC) [62] and cardiac tissue progenitors respond to injury with increased proliferation [60]. Many studies have demonstrated that stimulation of EC proliferation is associated with improved outcomes after experimental cardiac injury [21,27,45,55,58]. In contrast, increased proliferation of fibroblasts may induce a pathological fibrotic process [33,43]. Therefore, better understanding of molecular mechanisms involved in the regulation of cardiac cell type-specific proliferation is required for development of new therapeutic approaches to cure heart disease.

ErbB receptor tyrosine kinase signaling is critical for adult heart function [42] and repair after cardiac injury [4,20]. There are four ErbB receptor family members, including ErbB1 (also known as epidermal growth factor receptor or EGFR), ErbB2, ErbB3 and ErbB4. The ErbB2 is expressed in multiple cardiac cell types. ErbB2-mediated intracellular signaling is reliant upon heterodimerization with ErbB1, ErbB3 or ErbB4 as there is no natural ErbB2 ligand. Both ErbB2 and ErbB4 are found in cardiomyocytes. Neuregulin-dependent activation of ErbB2/4 signaling in cardiomyocytes results in protection against anthracycline- and ischemia-induced injuries [2,14,17]. ErbB2, ErbB3, and ErbB4 are expressed in endothelial cells and regulate angiogenic activity [19,53]. Several studies have demonstrated expression of all four ErbB receptors in cardiac fibroblasts, where they regulate proliferation and paracrine signaling [5,24,31].

We have previously shown that human ventricular myocardium contains a small population of cells which possess remarkable proliferative potential and could be identified by colony-forming ability [54]. Here we examined whether these cells can be isolated from epicardial biopsies and whether they express functional ErbB receptors. We found that human eHiPC express ErbB1-4 receptors that vary among individuals. Experimental studies characterizing baseline and ligand-activated proliferation and phenotype support the hypothesis that ErbB ligands and receptors function in eHiPC to regulate endothelial cell proliferation and phenotype.

* Corresponding author at: Maine Medical Center Research Institute, 81 Research Drive, Scarborough, ME 04074, United States.
E-mail address: DSawyer@mmc.org (D.B. Sawyer).

https://doi.org/10.1016/j.yjmcc.2017.12.013
Received 11 August 2017; Received in revised form 20 December 2017; Accepted 28 December 2017
Available online 29 December 2017
0022-2828/

Table 1
Baseline clinical characteristics of study population.

	All subjects (n = 15)
Age (years)	63.6 ± 3.3[a]
Female	13%
Male	87%
Body Mass Index	29.6 ± 1.3
A1C (%)	6.4 ± 0.4
Insulin	7%
Non-insulin antidiabetic agent	73%
ACE-inhibitor or ARB	47%
Beta-blocker	67%
Aspirin	27%
Statin	67%
LVEF < 50	N = 2
LVEF at least 50%	N = 13

[a] Data presented as mean ± SEM, unless otherwise indicated.

2. Methods

2.1. Subjects demographics

The study cohort consisted of 15 patients recruited to undergo intraoperative myocardial biopsy at the time of scheduled coronary artery bypass grafting surgery at Maine Medical Center (MMC) in Portland, Maine. All subjects provided informed consent approved by the MMC Institutional Review Board. All subjects were over 18 years of age. Subjects with known active myocarditis, hypertrophic cardiomyopathy, constrictive pericarditis, significant valvular and/or pericardial disease, severe pulmonary hypertension, significant hepatic disease or renal impairment (creatinine > 2.5 mg/dL), severe ventricular arrhythmias, malignancy other than non-melanoma skin cancers, expected survival less than one year and inability to provide informed consent were excluded. Demographic data are presented in Table 1.

2.2. Reagents

EBM-2 Basal Medium and EGM-2 SingleQuot Kit supplement/growth factors were purchased from Lonza Walkersville, Inc. (Walkersville, MD), and EGM Cell Growth Medium-2 was prepared according the manufacturer's instructions. NRG-1 (ECD, 377-HB) and EGF (236-EG) were purchased from Bio-Techne/R&D Systems. The recombinant human glial growth factor 2 (GGF2; neuregulin-1beta3; USAN - cimaglermin alfa) was provided by Acorda Therapeutics (Ardsley, NY). Calcein AM and 7-AAD were from ThermoFisher Scientific/Molecular probes. AG-1478 and TAK-165 were obtained from Tocris Bioscience (Bristol, UK). AST-1306 was purchased from SelleckChem (Houston, TX). Collagenase II (345 units/mg, CLS-2) was purchased from Worthington biochemical Corporation (Lakewood, NJ), dispase II (04942078001) was from Roche Life Science (Indianapolis, IN) and DNase I was from Sigma (St. Louis, MO). For experiments involving cell stimulation, final concentrations of dimethyl sulfoxide (Cell Culture grade, Sigma) did not exceed 0.1%.

2.3. LV epicardial biopsy

All procedures for tissue procurement were performed in compliance with institutional guidelines for human research and an institutional review board approved protocol at MMC. Anterior LV free wall epicardial biopsies (average weight 26.4 ± 1.8 mg) were obtained during planned coronary artery bypass surgery soon after the patient was placed on cardiopulmonary bypass, as described [11,65]. The epicardial biopsy was placed in serum-free DMEM medium and kept on wet ice. All samples were processed within 3 h of collection. All patients were followed post-operatively until discharge. No adverse effects or post-operative complications ascribable to the biopsy were detected, and all patients were discharged alive.

2.4. Preparation of cell suspension from LV epicardial biopsy

Isolation of cardiac stromal cell populations was performed according to a protocol published previously [54]. In brief, minced tissue was incubated in digestion solution (10 mg/ml collagenase II, 2.5 U/ml dispase II, 1 μg/ml DNase I, and 2.5 mM $CaCl_2$) for 45 min at 37 °C. After passing through a 70-μm cell strainer, the resulting myocyte-free single-cell suspension was centrifuged at 500 × *g*, washed with Dulbecco's PBS, and resuspended in PBS/0.5%BSA/2 mM EDTA. Cells were counted and the cell suspension was divided into two parts. One part was immediately used for flow cytometry analysis and the other part was used to isolate eHiPC.

2.5. Flow cytometric analysis

Cells (10^6/ml) were treated with Human TruStain FcX™ (Biolegend, San Diego, CA) to prevent non-specific binding followed by incubation with relevant antibodies for 25 min at 4 °C. Cell-surface antigen expression was examined using the following antibodies: FITC-conjugated CD45 (HI30), CD90 (Thy-1) and CD105 (43A3), PeCy7-conjugated CD73 (AD2) and CD309 (VEGFR2, 7D4-6), APC-conjugated CD29 (TS2/16), CD117 (c-Kit, 104D2) and CD202b (Tie2, 33.1(Ab33)), and APC/Cy7-conjugated CD31 (WM59) (all from BioLegend, San Diego, CA). FITC-conjugated CD34 (4H11) and CD49f-PeCy7 (eBioGoH3) were from eBioscience/Thermo Fisher Scientific.

ErbB receptors were assayed using PE-conjugated anti-human ErbB2 (Fab1129P) and IgG2b isotype-matched control (IC0041P), ErbB3 (Fab3481P) and IgG1 control (IC002P), ErbB4 (Fab11311P) and IgG2a (IC003P) isotype control. All anti-ERBB antibodies and controls were purchased from R&D Systems (Minneapolis, MN). All antibodies were titrated to establish high separation between positive and negative cell

Table 2
The effect of different cell densities on the number of eHiPC colonies and CD45 cells.

Number of cells seeded per well[a]	Number of wells	Number of colonies[b]	p value[‡]	Number of wells with both colony and non-colony cell expansion	p value[‡]	Number of colonies with $CD45^{pos}$ cells (% of CD45 cell)[c]
50	400	2.6 ± 0.5	–	0.6 ± 0.2	–	nd
100	200	3.2 ± 1.3	ns	1.0 ± 0.3	ns	nd
500	40	3.6 ± 0.9	ns	1.2 ± 0.4	ns	nd
1000	20	5.8 ± 1.2	p < 0.05	1.8 ± 0.4	p < 0.05	1.4 ± 0.7 (3.1 ± 1.2)
2000	10	8.2 ± 1.7	p < 0.05	8.8 ± 0.6	p < 0.001	4.0 ± 1.0 (5.8 ± 2.3)

Colony data represent mean ± SEM from five independent cell isolations (n = 5); nd – not detected.
[a] Cells were seeded in a 48 well culture dish with 1 cm^2 growth area.
[b] Number of colonies was determined on day 7.
[c] Percent of $CD45^{pos}$ cells was evaluated after colonies reached 100% confluence using flow cytometry.
[‡] p-values were calculated using an unpaired *t*-test in comparison to 50 cells/well; ns – not significant.

populations while maintaining a low level of background. Isotype-matched control antibodies were used to determine the level of undesired non-specific binding. Fluorescence spillover in multiparametric multicolor flow cytometric analysis was corrected after including all relevant antibodies in the other channels along with an isotype control antibody in a single channel of interest [34]. The expression of cell markers and ErbB receptors was determined after subtraction of the mean fluorescence intensity (MFI) of isotype-matched controls from the

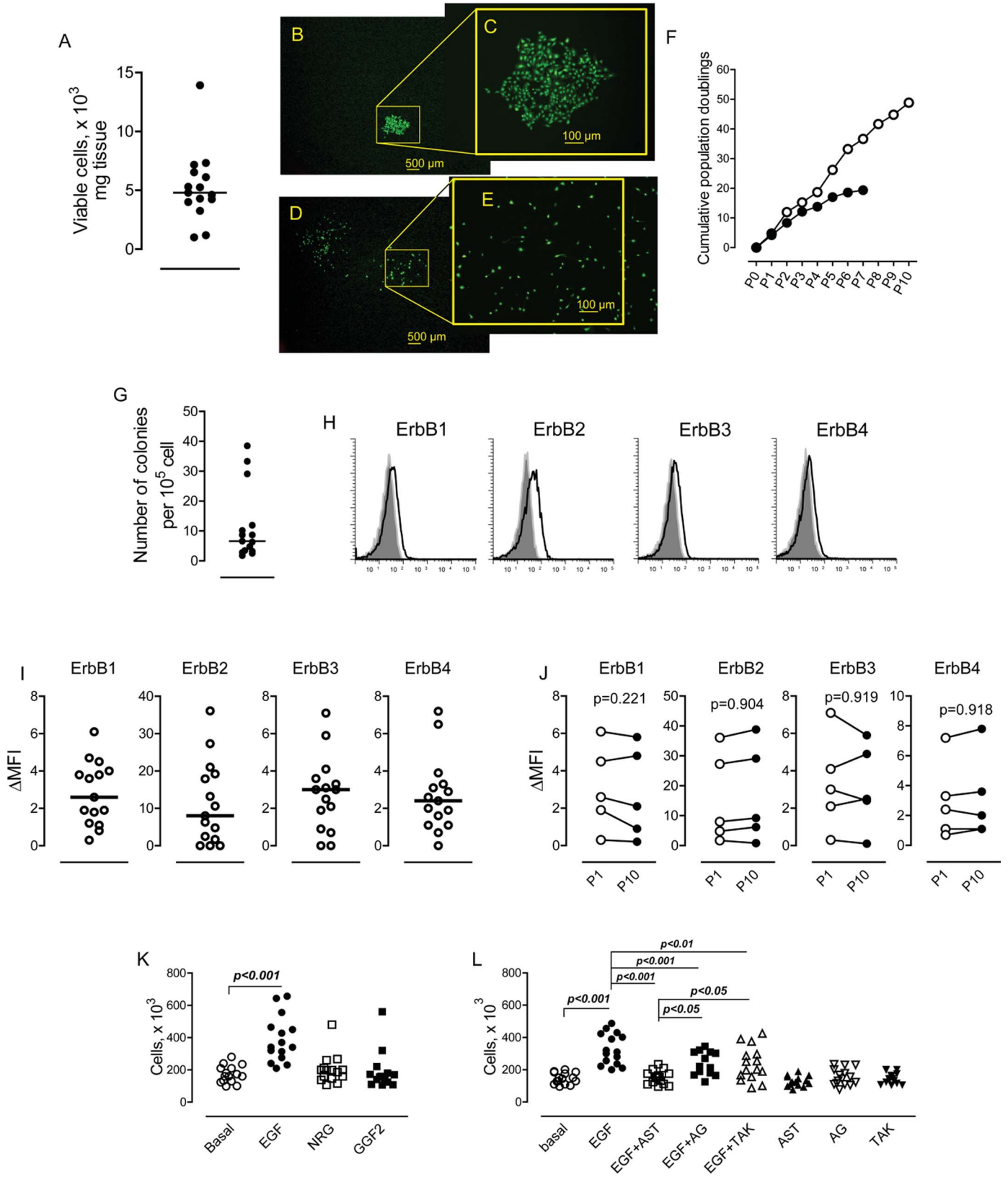

(caption on next page)

Fig. 1. Isolation and expansion of human epicardial eHiPC. Single cell suspensions prepared from LV epicardial biopsies were plated into 48 well plates at low cell density (500 cell/cm^2) and analyzed for growing colonies twice weekly. A. Number of viable cells per mg of LV biopsies. B–E. Micrographs of highly-proliferative colony-forming cells (B, C) and cells characterized by non-colony expansion (D, E). F. Comparison of proliferative potentials of colony-forming and non-colony forming cardiac cells. Cumulative number of population doublings was calculated by repeated cell number recordings in triplicate cultures at ~90% confluence and plating at a fixed number of 10^4 cells/cm^2 in 6 well plates. G. Average number of eHiPC colonies isolated from individual LV biopsies. H. Representative flow cytometric histograms showing cell surface expression of ErbB1-4 receptors; open histograms represent specific ErbB1-4 staining, shaded represent the isotype-matched IgG control. I. Graphical representation of ErbB1-4 receptor expression on HiPC; Data are expressed as ΔMFI and presented as scatter dot plots. ΔMFI was calculated by subtraction of the MFI corresponding to cells stained with isotype-matched control antibody from the MFI of the specific ErbB antibody. The median values (indicated by the horizontal lines) and individual values are shown. J. Expression of ErbB receptors was measured at passage 1 and passage 10 in five eHiPC clones as described in the text. Significance was calculated using a paired *t*-test. p values are indicated. K. Effects of recombinant ErbB ligands, 100 nM epidermal growth factor (EGF), 100 nM of neuregulin-1 (NRG) and 100 nM glial growth factor 2 (GGF2) on the proliferation of eHiPC. L. Effects of ErbB antagonists, 100 nM AST1306 (AST, a pan-ErbB inhibitor), 300 nM AG1478 (AG, ErbB1 inhibitor) and 300 nM TAK-165 (TAK, ErbB2 inhibitor) on the EGF-induced proliferation of HiPC; n = 15, One-way ANOVA, p-values for the Bonferroni post hoc test are indicated.

MFI of specific antibodies and represented as a delta mean fluorescence intensity (ΔMFI) as described elsewhere [18]. Data acquisition was performed on a MacsQuant Analyzer 10 (Miltenyi Biotec., Inc.) and the data were analyzed using WinList 5.0 software. When freshly isolated cardiac cells were analyzed, erythrocytes were lysed with ammonium chloride and small events (microparticles, platelets) were excluded from the analysis by setting a gate to exclude size < 6 μm using non-fluorescent size calibration microbeads (1,672,312, Life Technologies/Thermo Fisher Scientific). Viable and non-viable cells were distinguished using DAPI (to detect dead nucleated cells) and LIVE/DEAD® Fixable Violet Stain kit for detection of non-nucleated cell debris (Life Technologies, Carlsbad, CA).

2.6. Isolation and culture of eHiPC

To determine the optimal number of cells to produce colonies of eHiPC from LV epicardial biopsies, we seeded cells at different initial cell densities and determined the yield of colonies. Numbers of colonies were examined at 3, 7 and 14 days after isolation. We found no differences in the total number of colonies when cells were seeded at initial densities of 50, 100 or 500 cells/cm^2 (Table 2). Higher numbers of colonies were found when cell density was increased to 10^3 cells/cm^2 and 2×10^3 cells/cm^2. However, 24% and 49%, respectively, of these colonies generated from higher density plating contained CD45 positive cells indicating immune cell contamination. Also, we found non-colony cell expansion in almost every well with an initial cell density equal to or > 10^3 cells/cm^2, which made evaluation of single colony growth difficult. Based on these data, we used an initial cell density of 500 cells per cm^2 to produce colonies of eHiPC. Cells were grown using M199-EGM-2 (3:1, v/v) supplemented with 10% FBS and antibiotic-antimycotic solution (Sigma). The wells were analyzed for growing colonies twice weekly. Rapidly growing clones were harvested and resuspended in fresh growth medium at a density of 5×10^3 cells/cm^2. Cells were cultured under a humidified atmosphere of air/CO_2 (19:1) at 37 °C for one or two passages before using for experiments. One eHiPC colony per each LV epicardial biopsy was arbitrarily chosen for further analysis.

2.7. Matrigel-based tube formation assay

Clones of eHiPC cells (1.5×10^4 cells) were seeded on a layer of polymerized Growth Factor Reduced (GFR) Matrigel (BD Biosciences) in 96 well plate. Cells were incubated for 12 h under humidified atmosphere of air/CO_2 (19:1) at 37 °C. Tube formation was inspected under an inverted phase-contrast light Olympus IX-70 microscope equipped with a digital camera. Tube length was analyzed using ImageJ software (NIH, Bethesda, MD).

2.8. Collagen I-induced angiogenesis assay

Stimulation of cells with collagen I was performed as previously described [63] with minor modifications. In brief, cells were plated in 24 well plates at a density of 10^4 cells/cm^2 and grown to 100% confluence in a M199-EGM-2 growth medium. Twenty-four hours before stimulation, the culture medium was removed and replaced with a simplified 10% FBS M199-EBM-2 medium, depleted of growth factors. Acid solubilized rat tail collagen I (Corning, Bedford, MA) was neutralized by adding sodium bicarbonate to a concentration of 25 mM and diluted in serum-free M199-EBM-2 medium to a final concentration of 500 μg/ml. Culture medium was removed from the cell monolayer and washed once with PBS. Then cells were overlaid with collagen-containing serum-free medium and incubated for 3 h at 37 °C in a CO_2 incubator. Serum-free M199-EBM-2 medium (300 μl) was added to the well and incubated for an additional 9 h. At the end of the incubation (a total of 12 h), medium was removed and the collagen gel was released from the walls of the culture dish. Then 500 μl of serum-free M199-EBM-2 medium containing 2 μM Calcein AM and 5 μM 7-AAD were added to each well and incubated for 30 min. Fluorescence images (4 random fields per well) were collected with an Olympus IX70 microscope and analyzed using ImageJ (National Institutes of Health). Endothelial cell morphogenesis was quantified by measuring the total empty area in a given culture as previously described [56].

2.9. Permeability assay

Epicardial HiPC were plated at a density of 5×10^3 cells /Transwell unit (6.5 mm diameter, 0.4 μm pore size polycarbonate filter; Corning, Kennebunk, ME) and grown for 5 days to form a tight monolayer. Size-selective assessment of tight junction paracellular permeability was performed using 4 kDa fluorescein isothiocyanate (FITC)-dextran and 70 kDa rhodamine B isothiocyanate (RITC)-dextran (Sigma/Aldrich). In brief, medium was refreshed 1 h before the experiment, then 4 kDa FITC-dextran and 70 kDa RITC-dextran were added to the inner chamber to a final concentration of 1 mg/ml (for each tracer), and cells were incubated for 3 h in a 5% CO_2 incubator. Paracellular permeability was determined by measuring concentrations of fluorescent tracers in the outer chamber using a GloMax explorer system (Promega, Madison, WI).

2.10. Statistical analysis

Data were analyzed with GraphPad Prism 4.0 (GraphPad Software Inc., San Diego, CA). For normally distributed variables, comparisons between two groups were performed using two-tailed unpaired *t*-tests. Comparisons between several treatment groups were performed using one-way ANOVA followed by Bonferroni post hoc tests. Data are expressed as median values when distributions are skewed. For variables with skewed distributions, pairwise comparisons of median values were examined using the Mann Whitney test. Wilcoxon matched-pairs signed rank test was used to compare different subjects within a matched-pairs study design. A p-value < 0.05 was considered significant.

3. Results

3.1. ErbB1-4 receptors are expressed on eHiPC

Anterior LV free wall epicardial biopsies (average weight, 26 mg)

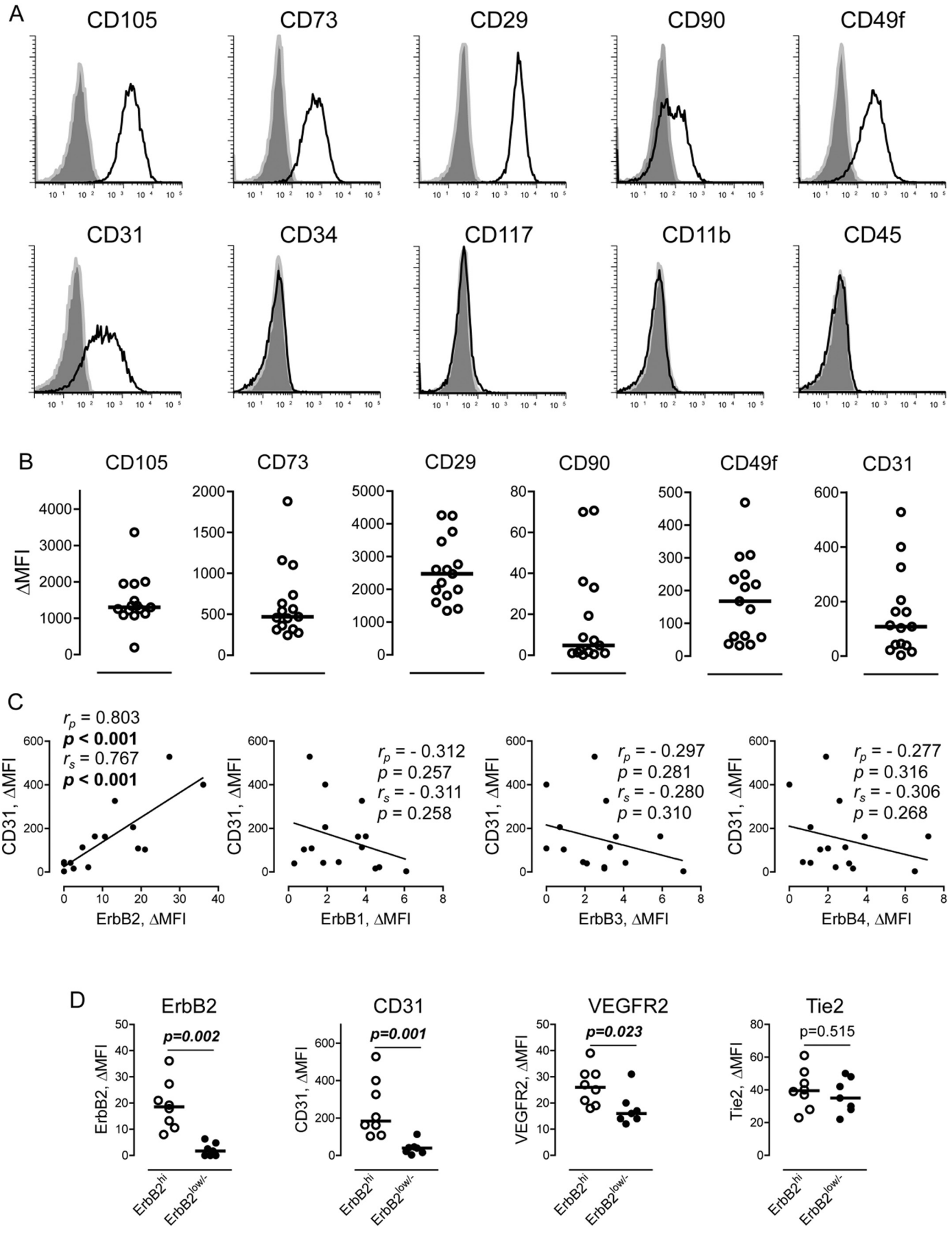

(caption on next page)

Fig. 2. Analysis of cell surface marker expression on eHiPC. A. Representative flow cytometric histograms demonstrating expression of mesenchymal stem cells and hematopoietic cell markers; open histograms represent antigen-specific IgGs and shaded ones represent isotype-matched IgGs. B. Graphical representation of flow cytometric data; horizontal lines indicate median values. C. Correlations between expression of ErbB1–4 receptors and CD31 (PECAM-1) on eHiPC; Pearson correlation coefficient (r_p), Spearman correlation coefficient (r_s), and p-values are shown. D. Cell surface expression of endothelial cell markers in groups of ErbB2^{high} and ErbB2^{low} eHiPC.

were used to obtain approximately 10^5 myocyte-depleted cardiac cells (Fig. 1A). These cells were seeded at low cell density (500 cells/cm^2) to produce colonies of highly proliferative cells. As expected, the cardiac cell suspension contained a mixture of colony-forming (Fig. 1B and C) and non-colony-forming cells (Fig. 1D and E). To characterize the proliferative capability of cardiac cells, we plated colony- and non-colony expanded cells at a density of 10,000 cells per cm^2, and the cultures were subsequently passaged. Colony-forming cells were capable of > 50 population doublings over ten passages (total time in culture 42.6 ± 1.4 days). In contrast, non-colony cells continued proliferating for only six passages, corresponding to approximately 20 population doublings (Fig. 1F).

The numbers of colony-forming eHiPC from cardiac cell suspensions obtained from each individual LV biopsy was characterized by moderate inter-individual variability (IIV) with a coefficient of quartile deviation value of 0.58 (Fig. 1G). After reaching 90% confluence, colonies of eHiPC were analyzed for the expression of ErbB1–4 receptor using flow cytometry. As shown in Fig. 1H, cell surface expression of all four ErbB receptors was found on eHiPC. The level of ErbB receptors varied among eHiPC obtained from different subjects. ErbB2 and ErbB3 showed highest IIV with calculated CQD values of 0.84 and 0.6 respectively (Fig. 1I) compared to ErbB1 and ErbB4 (CQD values: 0.53 and 0.5 respectively).

To determine the stability of ErbB receptor expression during in vitro passaging, we selected five clones with MFI values corresponding to minimum, first quartile, median, third quartile, and maximum levels of each ErbB receptor expression. These clones were maintained in culture for 10 passages and then used to determine level of ErbB receptors. As shown in Fig. 1J, the cell surface expression of ErbB1–4 receptors remained unchanged between passages 1 and 10, indicating the phenotypic stability of cultured eHiPC.

3.2. EGF/ErbB1 signaling promotes proliferation of eHiPC

The activation of ErbB-dependent signaling is known to be associated with accelerated proliferation and progenitor cell colony formation [32,50,57]. Stimulation of eHiPC with EGF, an ErbB1 ligand, increased cell proliferation (389.4 ± 36.7 vs. 172.9 ± 13.8 × 10^3 cell/cm^2, EGF vs. basal, Fig. 1K). In contrast, two isoforms of the ErbB3/4 ligand neuregulin-1β (an immunoglobulin domain-containing recombinant (NRG-1) and the kringle-domain containing glial growth factor-2 (GGF2)), had no effect on eHiPC proliferation. Accordingly, AG-1478, a potent and specific ErbB1 antagonist inhibited EGF induced proliferation (234.0 ± 17.9 vs. 328.1 ± 24.8 × 10^3 cell/cm^2, EGF and AG-1478 vs. EGF alone, Fig. 1L). In addition, the specific ErbB2 antagonist TAK-165 significantly attenuated the effect of EGF on eHiPC indicating that both ErbB1 and ErbB2 are involved in stimulation of proliferation (233.2 ± 26.9 vs. 328.1 ± 24.8 × 10^3 cell/cm^2, EGF and TAK-165 vs. EGF alone, Fig. 1L). A pan-ErbB receptor antagonist, AST-1306, demonstrated stronger inhibition compared to AG-1478 or TAK-165 (153.0 ± 10.8 vs. 234.0 ± 17.9 and 233.2 ± 26.9 × 10^3 cell/cm^2, AST-1306 vs. AG-1478 and TAK-165 respectively, Fig. 1L), further confirming that cooperation between ErbB1 and ErbB2 contributed to EGF-induced proliferation of eHiPC.

3.3. ErbB2 expression is associated with endothelial cell marker expression in eHiPC

To characterize cell surface phenotype, we performed flow cytometric analysis of cell surface markers expressed on eHiPC at passage 1. Immunophenotyping revealed the strong expression of CD105 (endoglin), CD73 (ecto-5′-nucleotidase) and CD29 (integrin β1), with undetectable expression of CD34, CD117 (c-kit), CD11b, and CD45 (Fig. 2A). This result is similar to the phenotype previously reported for mesenchymal stem-like and CD105^{pos} cardiac progenitor cells [10]. In addition, we found the presence of CD90 (Thy-1), CD49f (integrin alpha 6) and CD31 (PECAM-1) on eHiPC. However, the expression of these proteins was characterized by large IIV with CQD values of 0.62, 0.94 and 0.68, respectively (Fig. 2B). A strong positive correlation was found between CD31/PECAM-1 and ErbB2 but not ErbB1, ErbB3 or ErbB4 (Fig. 2C). No relationships were found between ErbB receptors and CD105, CD73, CD29, CD90 and CD49f (Supplemental Fig. 1).

CD31 is a pan-endothelial cell marker. To further investigate the association between ErbB2 and additional endothelial cell markers, we analyzed cell surface expression of vascular endothelial growth factor receptor 2 (VEGFR2) and receptor tyrosine kinase Tie2. As seen in Fig. 2D, colonies which expressed high levels of ErbB2 and CD31 were also characterized by higher expression of VEGFR2 compared to ErbB2^{low} cells. In contrast, no difference was found in the level of Tie2 expression between ErbB2^{high} and ErbB2^{low}- expressing colonies.

3.4. ErbB2^{high} eHiPC display higher endothelial-like morphogenic activity compared to ErbB2^{low} eHiPC

We tested the angiogenic properties of eHiPC using a Matrigel-based tube formation assay. As shown in Fig. 3A, pro-angiogenic extracellular matrix induced the formation of a characteristic tube network of both ErbB2^{high} and ErbB2^{low} eHiPC. The total tube length, however, was significantly higher in ErbB2high eHiPC compared to ErbB2low eHiPC (Fig. 3B). Collagen I, a major component of cardiac muscle ECM, provokes endothelial cell monolayer reorganization into cord-like structures, thus promoting formation of new vessels. We found that monolayers of ErbB2^{high} eHiPC underwent significant retraction and formation of cord-like structures in response to collagen I (Fig. 3C and D). In contrast, collagen I induced little or no morphogenic activity in ErbB2^{low} eHiPC (Fig. 3E, F and quantified in 3G). To test whether or not cell death is involved in the retraction of the ErbB2^{high} eHiPC monolayer, we performed staining of cells with Calcein AM and 7-AAD. As shown in Fig. 3H, viable cells were Calcein AM positive (green) and 7-AAD negative, while permeabilized cells were 7-AAD positive (red) and Calcein AM negative. Examination of monolayers revealed that retraction of ErbB2^{high} eHiPC cell monolayers is not due to cell death as the number of 7-AAD positive cells was not different between basal conditions and after stimulation with collagen I (Fig. 3I).

3.5. ErbB2^{high} eHiPC form a less permeable barrier compared to ErbB2^{low} eHiPC

To further characterize endothelial cell-like properties, we performed size-selective analysis of paracellular permeability. We found that diffusion of both 4 kDa and 70 kDa fluorescently labeled dextrans across ErbB2^{high} and ErbB2^{low} eHiPC was significantly reduced compared to empty filters (no cell monolayer). ErbB2^{high} eHiPC, however, formed less permeable monolayers compared to ErbB2^{low} eHiPC as indicated by significantly reduced diffusion of dextrans (Fig. 3J and K). The monolayer formed by ErbB2^{high} but not ErbB2^{low} eHiPC also restricted diffusion in a size selective manner, indicating formation of functional tight junctions (Fig. 3L).

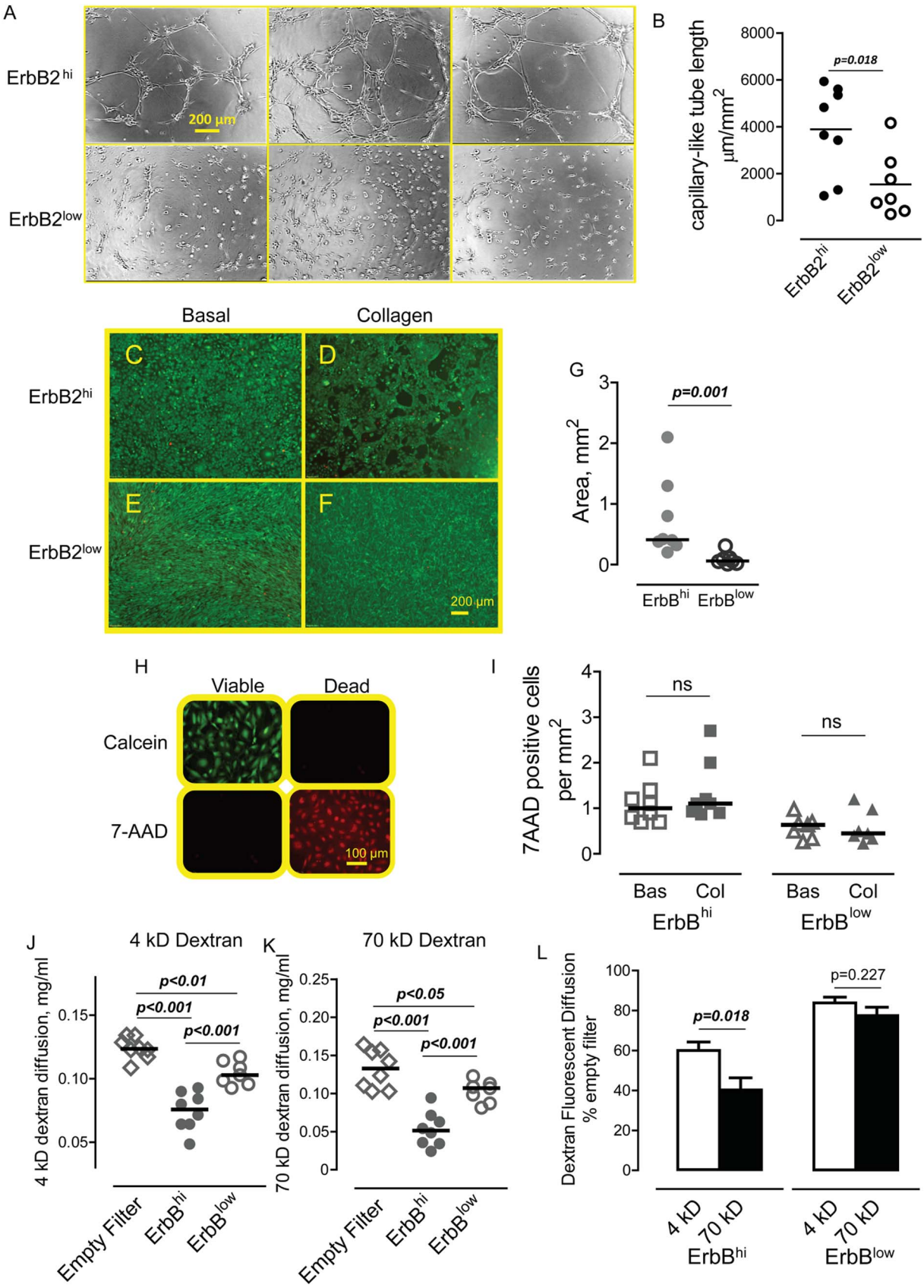

(caption on next page)

Fig. 3. Assessment of endothelial cell-like properties of ErbB2^{high} and ErbB2^{low} eHiPC. In vitro angiogenic properties were examined using growth factor reduced Matrigel (A-B) and after stimulation of eHiPC with collagen I (C-G). Barrier function was measured by paracellular permeability of fluorescently labeled 4 kDa and 70 kDa dextrans (H-L). Representative microscopic fields (A) and graphical representation (B) of data showing Matrigel-based tube formation by ErbB2^{high} (ErbB2^{hi}, upper panel) and ErbB2^{low} (lower panel) eHiPC, unpaired *t*-test. C,D. Representative microscopic fields demonstrating cell retraction and reorganization of the monolayer of ErbB2^{high} eHiPC into cord-like structures at 12 h after addition of 500 μg/ml collagen I. E, F. In contrast, ErbB2^{low} eHiPC did not undergo morphogenesis. Bar = 200 μm. G. Graphical representation of total empty area after collagen I–induced morphogenic activity within cultures shown in C–F. Graphs are presented as scatter dot plots and the horizontal lines indicate the median values for each group. Each dot represents averaged total empty area from four fields per well (two wells per colony) normalized to mm^2. Significance level (p-value) calculated by Mann Whitney test. H. Calcein AM and 7-AAD were used to determine number of dead cells (7-AAD positive/Calcein AM negative); the upper left panel represents viable cells, the lower right panel represents dead cells (0.5% Tween 20). I. Number of dead cells under basal (Bas) and collagen I (Col)-induced conditions; ns is not significant, Mann Whitney test. J–L. Diffusive paracellular permeability of 4 kDa (J) and 70 kDa (K) dextrans. Permeability was measured at a 3 h time point in triplicate per individual eHiPC colony and averaged. Empty filter indicates no cells. Horizontal lines demonstrate mean values. One-way ANOVA, p-values determined by Bonferroni's posttest. L. Paracellular diffusion of 4 kDa and 70 kDa dextrans through eHiPC monolayers was normalized to diffusion across empty filters, unpaired *t*-test.

3.6. ErbB ligands promote upregulation of endothelial cell markers CD31/PECAM-1, VEGFR2, and Tie2 on eHiPC

We compared the effects of ErbB ligands on endothelial marker expression in groups of ErbB2^{high} and ErbB2^{low} eHiPC. We found that EGF, NRG-1 (NRG) and GGF2 promote upregulation of CD31 cell surface expression in ErbB2^{high} eHiPC (Fig. 4A and B). The effect of EGF was stronger than that of NRG-1 or GGF2, which induced similar levels of CD31 expression. In contrast, we found no effects of ErbB ligands in a majority of ErbB2^{low} eHiPC (Fig. 4C). As shown in Fig. 4D, a pan-ErbB inhibitor (AST-1306) and an ErbB1 inhibitor (AG-1478) abolished EGF-mediated upregulation of CD31 in ErbB2^{high} eHiPC (234.1 ± 15.0 and 259.8 ± 23.1 vs. 357.8 ± 31.1 ΔMFI, AST-1306 and AG-1478 in combination with EGF vs. EGF alone). An ErbB2 inhibitor (TAK-165) alone suppressed the EGF-induced increase in CD31 expression (260.4 ± 21.0 vs 357.8 ± 31.1 ΔMFI, TAK and EGF vs. EGF alone, Fig. 4D) to a similar degree as AST-1306 and AG-1478. Thus it appears that ErbB2 is required for ErbB-associated regulation of CD31 in eHiPC.

In contrast to CD31, EGF but not NRG-1 or GGF2 increased VEGFR2 expression on both ErbB2^{high} and ErbB2^{low} eHiPC (38.8 ± 4.3 vs. 22.3 ± 2.1 ΔMFI, EGF vs. basal, Fig. 4E and F). Furthermore we found that AST-1306 and AG-1478 but not TAK-165 prevented the effect of EGF-dependent upregulation of VEGFR2 expression (21.4 ± 1.9 and 23.9 ± 2.4 vs. 38.8 ± 4.3 ΔMFI, AST-1306 and AG-1478 in combination with EGF vs. EGF alone, Fig. 4G). Thus ErbB1 receptor activation is sufficient to induce upregulation of cell surface expression of VEGFR2 in eHiPC.

As shown in Fig. 4H and I, all three ligands induced upregulation of Tie2 on eHiPC to a similar degree, irrespective of ErbB2 expression. Both AST-1306 and AG-1478, but not TAK-165, were effective in the inhibition of EGF-induced Tie2 expression (40.1 ± 2.3 and 41.6 ± 2.6 vs. 55.5 ± 3.7 ΔMFI, AST-1306 and AG-1478 in combination with EGF vs. EGF alone, Fig. 4J). However, only the pan-ErbB inhibitor AST-1306 but not AG-1478 or TAK165 abolished the effect of NRG-1 (39.2 ± 3.1 vs. 55.3 ± 4.5 ΔMFI, AST-1306 in combination with NRG-1 vs. NRG-1 alone, Fig. 4K) and GGF2 (33.9 ± 3.9 vs. 58.7 ± 2.2 ΔMFI, AST-1306 in combination with GGF2 vs. GGF2 alone, Fig. 4L). These data suggested that ErbB1 and ErbB3/4 receptors are sufficient to induce upregulation of Tie2 on eHiPC.

3.7. The number of endothelial cells in LV epicardial biopsies is higher in subjects with high expression of ErbB2 on eHiPC

Freshly isolated cell suspensions were analyzed to determine the number of endothelial cells in LV epicardial biopsies obtained from subjects with high and low expression of ErbB2 on eHiPC using flow cytometry. Endothelial cells were defined as CD31 positive cells within the CD45 negative (non-immune) cell population and represented a minor fraction of total isolated cells (Fig. 5A). We found that cell suspensions obtained from subjects with ErbB2^{high} eHiPC were characterized by comparatively higher percentages of CD31 positive endothelial cells than from subjects with ErbB2^{low} eHiPC. There was no difference in the total number of cells (Fig. 5B). However, the number of CD31^{pos}CD45^{neg} endothelial cells was higher in subjects with ErbB2^{high} eHiPC compared to ErbB2^{low} eHiPC subjects (Fig. 5C).

4. Discussion

Our main findings are that human eHiPC express functional ErbB1-4 receptors and that ErbB2 signaling contributes to the promotion of an endothelial phenotype. Previously, expression of ErbB receptors has been shown in many different cardiac cell types, including cardiac myocytes, endothelial cells, fibroblasts, and cardiac macrophages [15]. However, the expression of ErbB receptors and their role in cardiac cells with high proliferative potential has not been previously described. We have previously reported that human heart contains a subpopulation of cells with high proliferative potential and the capacity to differentiate into different cell types [54]. Here, we demonstrated that activation of variable expression of ErbB receptors on eHiPC determines their proliferative and differentiation potential, at least along the endothelial lineage. It appears that the subset of eHiPC with the highest ErbB2 expression represents a population of endothelial precursor cells and that ErbB ligands give distinct signals to these cells, reflecting their different ErbB complements. These findings expand our understanding of the role of ErbB signaling in the human heart, and have a number of implications.

The increased proliferative response from cardiac fibroblasts, endothelial cells and progenitors is essential for cardiac repair after heart injury. Recently, the role of ErbB2, ErbB3, and ErbB4 receptors in the stimulation of proliferation of normal human cardiac ventricular fibroblasts has been demonstrated [24]. In our current study, we found that EGF, acting via ErbB1 and ErbB2, stimulated proliferation of eHiPC. While ErbB2 signaling is strongly associated with cardioprotection [6,44], ErbB1-mediated signaling contributes to both pro-reparative (e.g. angiogenesis [36]) and adverse remodeling processes [39,47,59]. Further studies examining the role of eHiPC in cardiac disorders will help to investigate the effect of ErbB1/2-dependent activation of eHiPC proliferation. Surprisingly, we found no effect of NRG-1 or GGF2 on eHiPC proliferation. One potential explanation is that ErbB3 and ErbB4 receptors are expressed at a low level which is not sufficient for the activation of eHiPC proliferation.

One of the most interesting and novel findings from our study is related to the association of ErbB2 expression with an endothelial phenotype of eHiPC. Besides its role as a pan-endothelial marker, CD31 signaling is involved in the maintenance of vascular integrity [49], endothelial cell migration, angiogenesis, and survival [9,16,22]. Our data show that ErbB2^{high}CD31^{high} eHiPC are characterized by higher proangiogenic and barrier properties compared to ErbB2^{low} eHiPC which express a low CD31 level. Our study provides new evidence for the role of ErbB2 signaling in directing eHiPC toward an endothelial lineage in adult hearts. Thus, we found that the number of CD31 endothelial cells in biopsies obtained from subjects with ErbB2^{high} eHiPC is higher compared to subjects with ErbB2^{low} eHiPC. Recently, a new role of ErbB2 in the coronary vasculature was described [1]. ErbB2 interacts with neuropilin-1 to form the Sema3d co-receptor required for proper formation of coronary veins in developing hearts. Because

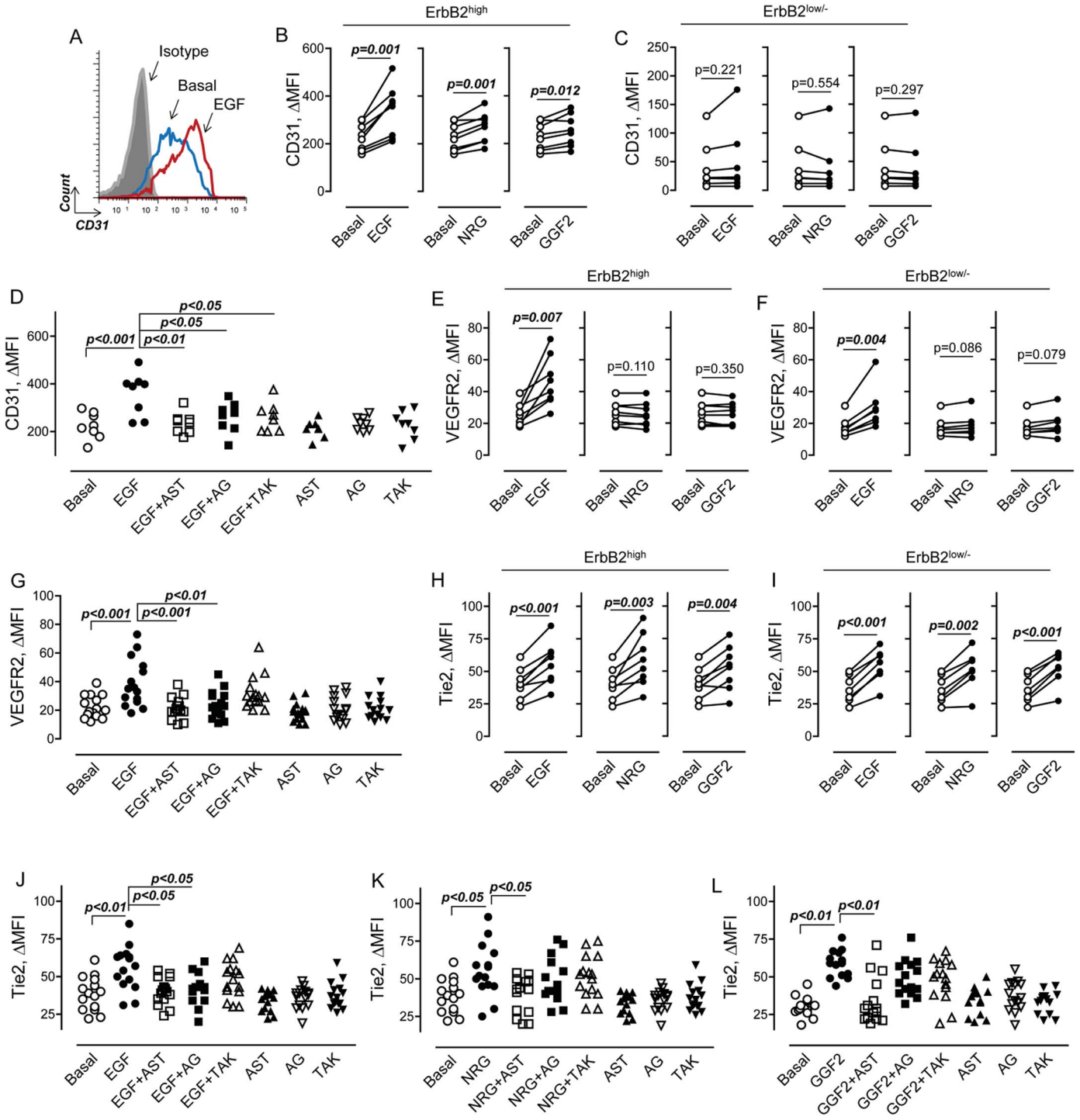

Fig. 4. ErbB ligands, EGF, NRG-1 and GGF2 upregulate cell surface expression of endothelial cell markers. Progenitors were serum-starved for 24 h and then incubated in the absence (Basal) or presence of 100 ng/ml of EGF, 100 ng/ml of NRG-1 (NRG) or 100 ng/ml of GGF2 for 48 h. A. Representative flow cytometric histograms showing the effect of EGF (red) on cell surface expression of CD31. B,C. Graphical representation of the effects of ErbB ligands on CD31 expression in ErbB^{high} (n = 8) (B) and ErbB2^{low} (n = 7) (C) eHiPC, paired *t*-test. D. Effect of ErbB receptor antagonists on CD31 expression in five colonies with high response to EGF, one-way ANOVA, p-values for the Bonferroni post hoc test are indicated. E, F. Effect of ErbB agonists on cell surface expression of VEGFR2 in ErbB^{high} (E) and ErbB^{low} (F) eHiPC; paired *t*-test. G. Effect of ErbB receptor antagonists on VEGFR2 cell surface expression; one-way ANOVA, p-values are indicated (Bonferroni's multiple comparison test). H,I. Effect of ErbB agonists on cell surface expression of Tie2 in ErbB^{high} (H) and ErbB^{low} (I) eHiPC; paired *t*-test. J-L. Effect of ErbB receptor antagonists on Tie2 cell surface expression in cells stimulated with EGF (J), NRG-1 (K) or GGF2 (L); one-way ANOVA, p-values are indicated (Bonferroni's multiple comparison test). (For interpretation of the references to colour in this figure legend, the reader is referred to the web version of this article.)

neuropilin-1 is expressed in endothelial precursors and promotes their endothelial phenotype, it would be interesting to understand whether ErbB2 and neuropilin-1 interactions play a role in the maintenance of microvasculature of the adult heart.

We also found that EGF/ErbB1 signaling is involved in the upregulation of VEGFR2, the main VEGF receptor on endothelial cells. VEGFR2 is crucial for endothelial cell biology during development and in the adult, as it regulates angiogenesis and vascular permeability [25]. Several studies have demonstrated that ErbB1 induces upregulation of VEGF [61]. Our data indicate that ErbB1 activation can increase

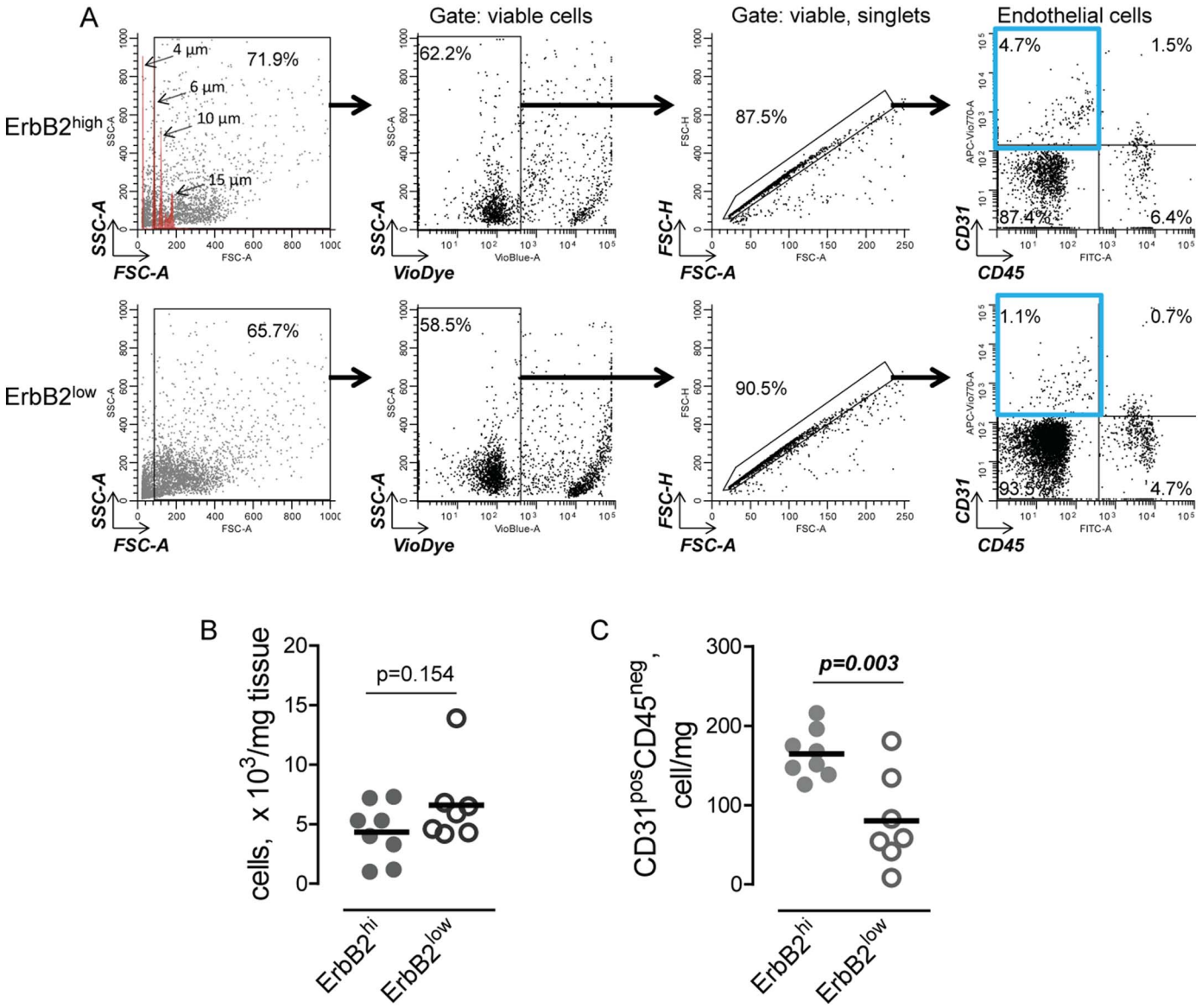

Fig. 5. Endothelial cell number is higher in LV epicardial biopsies obtained from subjects with ErbB2^{high} eHiPC compared to subjects with ErbB2^{low} eHiPC. A. Representative flow cytometric dot plots demonstrating the percentage of endothelial cells in cell suspensions prepared from LV epicardial biopsies obtained from subjects with ErbB2^{high} eHiPC (*upper panel*) and ErbB^{low} eHiPC (*lower panel*). Microbeads were used to gate events with size higher than 6 µm (*SSC-A/FSC-A, upper panel, left plot*). Dead cells and cell debris were excluded using amine-reactive dye (*VioDye, LIVE/DEAD® Fixable Dead Cell kit*) and cell aggregates were excluded using FSC-H/FSC-A. Endothelial cells (*blue gate, right plot*) were defined as CD31^{pos}CD45^{neg} cells. B. Number of viable cells obtained from LV epicardial biopsies of subjects with ErbB2^{high} and ErbB2^{low} eHiPC; unpaired *t*-test. C. Number of EC in the epicardium of subjects with high and low expression of ErbB2 on eHiPC; number of EC was calculated using percent of CD31^{pos}CD45^{neg} cells and total number of cells; unpaired *t*-test. (For interpretation of the references to colour in this figure legend, the reader is referred to the web version of this article.)

cell surface expression of VEGFR2, supporting a model where EGF pretreatment can increase the sensitivity of eHiPC to proangiogenic stimulation. This result might also explain the high expression of VEGFR2 on cells expressing a high level of ErbB1 [52].

Our data indicate that ErbB signaling also regulates expression of the angiopoietin receptor Tie2 on eHiPC. Angiopoetin-1 contributes to angiogenesis and survival of endothelial cells [8,23,46]. In contrast to another potent proangiogenic factor, VEGF, Ang-1/Tie2 signaling contributes to the stabilization and maturation of growing vasculature and to decreased vascular permeability [8]. Tie2 expression was upregulated to a similar extent by EGF, NRG-1 and GGF2. Recently, recombinant GGF2 have been shown to induce sustained beneficial improvement in cardiac function in subjects with heart failure [30]. Thus, the current data suggest that a possible effect on cardiac vasculature should be considered among the mechanisms for this effect of NRGs.

Cardiomyopathy is one of the major side effects of targeted therapy for ErbB2-positive cancers [7]. Although the exact mechanisms are still under investigation, the published data indicate that inhibition of ErbB2 results in increased generation of reactive oxygen species [28,41], downregulation of pro-survival PI3K/AKT signaling [48] and improper functioning of excitation–contraction coupling machinery and loss of contractile function [44]. Recently, we have shown that endothelial cells represent one of the major subpopulations of proliferating cells in the adult heart [3], indicating endothelial renewal in vivo. Our current findings suggest that ErbB2-targeted therapy may prevent endothelial differentiation of highly proliferative cells and perhaps contribute to endothelial dysfunction and development of cardiomyopathy [29].

One of the potential uses of highly proliferative cardiac cells is to generate high numbers of cells with pro-reparative properties in vitro, from a small amount of cardiac tissue obtained by biopsy, and reimplant these cells to promote cardiac repair. Thus, cardiosphere-

derived CD105^{pos} cells have been selected for their high rates of proliferation from endomyocardial biopsies [38,40]. These cells exhibited higher potency in restoring ventricular function post-MI [37]. Currently, these cells are being investigated in clinical trials as potential candidates for cell therapy [35,38]. Our data suggest that stimulation of ErbB2 expression on cardiac-derived highly proliferative cells may increase their therapeutic potential to promote revascularization. More research is needed to fully evaluate this hypothesis.

In summary, we demonstrate that human eHiPC express all four subtypes of ErbB receptors. The expression of ErbB receptor subtypes is characterized by large inter-individual variability. Our data demonstrate that eHiPC cells evoke diverse responses depending on the level of specific subtypes of ErbB receptor expression. These data suggest that ErbB receptor expression profile may predetermine the biological fate of eHiPC and their contribution to cardiac repair through promotion of an eHiPC endothelial phenotype.

Acknowledgments

This work was supported by the National Heart, Lung, and Blood Institute of the National Institutes of Health (P20 HL101425, U01 HL100398, F32HL136076, and R01 HL136560-01A1). We have also received support from the National Institute of General Medical Sciences funded COBRE in Stem and Progenitor Cell Biology and Regenerative Medicine (P30GM106391), COBRE in Vascular Biology (P30GM103392, and the Northern New England Clinical and Translational Research Network (U54115516). The content is solely the responsibility of the authors and does not necessarily represent the official views of the National Institutes of Health. This work was also supported by the American Heart Association (17POST33410474, 17MCPRP33660844) and a grant from Acorda Therapeutics, Inc. We are grateful to Joanne S. Burgess and Susan Bosworth-Farrell for subject recruitment and providing logistical support during sample collection, and the MMC BioBank, a Core Facility.

Appendix A. Supplementary data

Supplementary data to this article can be found online at https://doi.org/10.1016/j.yjmcc.2017.12.013.

References

[1] H. Aghajanian, Y.K. Cho, L.J. Manderfield, M.R. Herling, M. Gupta, V.C. Ho, L. Li, K. Degenhardt, A. Aharonov, E. Tzahor, J.A. Epstein, Coronary vasculature patterning requires a novel endothelial ErbB2 holoreceptor, Nat. Commun. 7 (2016) 12038.

[2] S. Akhtar, M.H. Yousif, B. Chandrasekhar, I.F. Benter, Activation of EGFR/ERBB2 via pathways involving ERK1/2, P38 MAPK, AKT and FOXO enhances recovery of diabetic hearts from ischemia-reperfusion injury, PLoS One 7 (2012) e39066.

[3] M.A. Asson-Batres, S.V. Ryzhov, O. Tikhomirov, C.W. Duarte, C. Bates Congdon, C.R. Lessard, S. McFarland, C. Rochette-Egly, T.L. Tran, C.L. Galindo, A.J. Favreau-Lessard, D.B. Sawyer, Effects of vitamin A deficiency in the postnatal mouse heart - role of hepatic retinoid stores, Am. J. Physiol. Heart Circ. Physiol. 00887 (2016) 2015.

[4] K. Bersell, S. Arab, B. Haring, B. Kuhn, Neuregulin1/ErbB4 signaling induces cardiomyocyte proliferation and repair of heart injury, Cell 138 (2009) 257–270.

[5] C.H. Chen, T.H. Cheng, H. Lin, N.L. Shih, Y.L. Chen, Y.S. Chen, C.F. Cheng, W.S. Lian, T.C. Meng, W.T. Chiu, J.J. Chen, Reactive oxygen species generation is involved in epidermal growth factor receptor transactivation through the transient oxidization of Src homology 2-containing tyrosine phosphatase in endothelin-1 signaling pathway in rat cardiac fibroblasts, Mol. Pharmacol. 69 (2006) 1347–1355.

[6] S.A. Crone, Y.-Y. Zhao, L. Fan, Y. Gu, S. Minamisawa, Y. Liu, K.L. Peterson, J. Chen, R. Kahn, G. Condorelli, J. Ross Jr., K.R. Chien, K.-F. Lee, ErbB2 is essential in the prevention of dilated cardiomyopathy, Nat. Med. 8 (2002) 459–465.

[7] M.S. Ewer, M.T. Vooletich, J.B. Durand, M.L. Woods, J.R. Davis, V. Valero, D.J. Lenihan, Reversibility of trastuzumab-related cardiotoxicity: new insights based on clinical course and response to medical therapy, J. Clin. Oncol 23 (31) (2005) 7820–7826.

[8] C. Daly, V. Wong, E. Burova, Y. Wei, S. Zabski, J. Griffiths, K.M. Lai, H.C. Lin, E. Ioffe, G.D. Yancopoulos, J.S. Rudge, Angiopoietin-1 modulates endothelial cell function and gene expression via the transcription factor FKHR (FOXO1), Genes Dev. 18 (2004) 1060–1071.

[9] H.M. DeLisser, M. Christofidou-Solomidou, R.M. Strieter, M.D. Burdick, C.S. Robinson, R.S. Wexler, J.S. Kerr, C. Garlanda, J.R. Merwin, J.A. Madri, S.M. Albelda, Involvement of endothelial PECAM-1/CD31 in angiogenesis, Am. J. Pathol. 151 (1997) 671–677.

[10] M. Dominici, K. Le Blanc, I. Mueller, I. Slaper-Cortenbach, F. Marini, D. Krause, R. Deans, A. Keating, D. Prockop, E. Horwitz, Minimal criteria for defining multipotent mesenchymal stromal cells. The International Society for Cellular Therapy position statement, Cytotherapy 8 (2006) 315–317.

[11] C. Donaldson, D.J. Taatjes, M. Zile, B. Palmer, P. VanBuren, F. Spinale, D. Maughan, M. Von Turkovich, N. Bishop, M.M. LeWinter, Combined immunoelectron microscopic and computer-assisted image analyses to detect advanced glycation end-products in human myocardium, Histochem. Cell Biol. 134 (2010) 23–30.

[12] D. Fan, A. Takawale, J. Lee, Z. Kassiri, Cardiac fibroblasts, fibrosis and extracellular matrix remodeling in heart disease, Fibrogenesis Tissue Repair 5 (2012) 15.

[13] N.G. Frangogiannis, L.H. Michael, M.L. Entman, Myofibroblasts in reperfused myocardial infarcts express the embryonic form of smooth muscle myosin heavy chain (SMemb), Cardiovasc. Res. 48 (2000) 89–100.

[14] R. Fukazawa, T.A. Miller, Y. Kuramochi, S. Frantz, Y.D. Kim, M.A. Marchionni, R.A. Kelly, D.B. Sawyer, Neuregulin-1 protects ventricular myocytes from anthracycline-induced apoptosis via erbB4-dependent activation of PI3-kinase/Akt, J. Mol. Cell. Cardiol. 35 (2003) 1473–1479.

[15] C.L. Galindo, S. Ryzhov, D.B. Sawyer, Neuregulin as a heart failure therapy and mediator of reverse remodeling, Curr. Heart Fail. Rep. 11 (2014) 40–49.

[16] C. Gao, W. Sun, M. Christofidou-Solomidou, M. Sawada, D.K. Newman, C. Bergom, S.M. Albelda, S. Matsuyama, P.J. Newman, PECAM-1 functions as a specific and potent inhibitor of mitochondrial-dependent apoptosis, Blood 102 (2003) 169–179.

[17] L.I. Gordon, M.A. Burke, A.T. Singh, S. Prachand, E.D. Lieberman, L. Sun, T.J. Naik, S.V. Prasad, H. Ardehali, Blockade of the erbB2 receptor induces cardiomyocyte death through mitochondrial and reactive oxygen species-dependent pathways, J. Biol. Chem. 284 (2009) 2080–2087.

[18] M.Y. Hardy, A.J. Kassianos, A. Vulink, R. Wilkinson, S.L. Jongbloed, D.N. Hart, K.J. Radford, NK cells enhance the induction of CTL responses by IL-15 monocyte-derived dendritic cells, Immunol. Cell Biol. 87 (2009) 606–614.

[19] N. Hedhli, Q. Huang, A. Kalinowski, M. Palmeri, X. Hu, R.R. Russell, K.S. Russell, Endothelium-derived neuregulin protects the heart against ischemic injury, Circulation 123 (2011) 2254–2262.

[20] M.F. Hill, A.V. Patel, A. Murphy, H.M. Smith, C.L. Galindo, L. Pentassuglia, X. Peng, C.G. Lenneman, O. Odiete, D.B. Friedman, M.W. Kronenberg, S. Zheng, Z. Zhao, Y. Song, F.E. Harrell Jr., M. Srinivas, A. Ganguly, J. Iaci, T.J. Parry, A.O. Caggiano, D.B. Sawyer, Intravenous glial growth factor 2 (GGF2) isoform of neuregulin-1beta improves left ventricular function, gene and protein expression in rats after myocardial infarction, PLoS One 8 (2013) e55741.

[21] X. Hou, H. Zeng, X. He, J.X. Chen, Sirt3 is essential for apelin-induced angiogenesis in post-myocardial infarction of diabetes, J. Cell. Mol. Med. 19 (2015) 53–61.

[22] C.S. Kim, T. Wang, J.A. Madri, Platelet endothelial cell adhesion molecule-1 expression modulates endothelial cell migration in vitro, Lab. Investig. 78 (1998) 583–590.

[23] I. Kim, H.G. Kim, J.N. So, J.H. Kim, H.J. Kwak, G.Y. Koh, Angiopoietin-1 regulates endothelial cell survival through the phosphatidylinositol 3'-kinase/Akt signal transduction pathway, Circ. Res. 86 (2000) 24–29.

[24] A. Kirabo, S. Ryzhov, M. Gupte, S. Sengsayadeth, R.J. Gumina, D.B. Sawyer, C.L. Galindo, Neuregulin-1β induces proliferation, survival and paracrine signaling in normal human cardiac ventricular fibroblasts, J. Mol. Cell. Cardiol. 105 (2017) 59–69.

[25] S. Koch, L. Claesson-Welsh, Signal transduction by vascular endothelial growth factor receptors, Cold Spring Harb. Perspect. Med. 2 (2012) (a006502).

[26] N. Koitabashi, D.A. Kass, Reverse remodeling in heart failure—mechanisms and therapeutic opportunities, Nat. Rev. Cardiol. 9 (2011) 147–157.

[27] C. Kupatt, J. Horstkotte, G.A. Vlastos, A. Pfosser, C. Lebherz, M. Semisch, M. Thalgott, K. Buttner, C. Browarzyk, J. Mages, R. Hoffmann, A. Deten, M. Lamparter, F. Muller, H. Beck, H. Buning, P. Boekstegers, A.K. Hatzopoulos, Embryonic endothelial progenitor cells expressing a broad range of proangiogenic and remodeling factors enhance vascularization and tissue recovery in acute and chronic ischemia, FASEB J. 19 (2005) 1576–1578.

[28] Y. Kuramochi, G.M. Cote, X. Guo, N.K. Lebrasseur, L. Cui, R. Liao, D.B. Sawyer, Cardiac endothelial cells regulate reactive oxygen species-induced cardiomyocyte apoptosis through neuregulin-1beta/erbB4 signaling, J. Biol. Chem. 279 (2004) 51141–51147.

[29] K. Lemmens, V.F. Segers, M. Demolder, G.W. De Keulenaer, Role of neuregulin-1/ErbB2 signaling in endothelium-cardiomyocyte cross-talk, J. Biol. Chem. 281 (2006) 19469–19477.

[30] D.J. Lenihan, S.A. Anderson, C.G. Lenneman, E. Brittain, J.A.S. Muldowney, L. Mendes, P.Z. Zhao, J. Iaci, S. Frohwein, R. Zolty, A. Eisen, D.B. Sawyer, A.O. Caggiano, A phase I, single ascending dose study of cimaglermin alfa (neuregulin 1β3) in patients with systolic dysfunction and heart failure, JACC: Basic to Translat. Sci. 1 (2016) 576–586.

[31] C.C. Lin, C.S. Pan, C.Y. Wang, S.W. Liu, L.D. Hsiao, C.M. Yang, Tumor necrosis factor-alpha induces VCAM-1-mediated inflammation via c-Src-dependent transactivation of EGF receptors in human cardiac fibroblasts, J. Biomed. Sci. 22 (53) (2015).

[32] S.A. Louis, R.L. Rietze, L. Deleyrolle, R.E. Wagey, T.E. Thomas, A.C. Eaves, B.A. Reynolds, Enumeration of neural stem and progenitor cells in the neural colony-forming cell assay, Stem Cells 26 (2008) 988–996.

[33] T. Lv, Y. Du, N. Cao, S. Zhang, Y. Gong, Y. Bai, W. Wang, H. Liu, Proliferation in cardiac fibroblasts induced by β1-adrenoceptor autoantibody and the underlying mechanisms, Sci. Rep. 6 (2016) 32430.

[34] H.T. Maecker, J. Trotter, Flow cytometry controls, instrument setup, and the

determination of positivity, Cytometry A 69 (2006) 1037–1042.
[35] R.R. Makkar, R.R. Smith, K. Cheng, K. Malliaras, L.E. Thomson, D. Berman, L.S. Czer, L. Marban, A. Mendizabal, P.V. Johnston, S.D. Russell, K.H. Schuleri, A.C. Lardo, G. Gerstenblith, E. Marban, Intracoronary cardiosphere-derived cells for heart regeneration after myocardial infarction (CADUCEUS): a prospective, randomised phase 1 trial, Lancet 379 (2012) 895–904.
[36] N. Makki, K.W. Thiel, F.J. Miller Jr., The epidermal growth factor receptor and its ligands in cardiovascular disease, Int. J. Mol. Sci. 14 (2013) 20597–20613.
[37] K. Malliaras, R.R. Makkar, R.R. Smith, K. Cheng, E. Wu, R.O. Bonow, L. Marban, A. Mendizabal, E. Cingolani, P.V. Johnston, G. Gerstenblith, K.H. Schuleri, A.C. Lardo, E. Marban, Intracoronary cardiosphere-derived cells after myocardial infarction: evidence of therapeutic regeneration in the final 1-year results of the CADUCEUS trial (CArdiosphere-derived aUtologous stem CElls to reverse ventricULar dySfunction), J. Am. Coll. Cardiol. 63 (2014) 110–122.
[38] E. Marban, E. Cingolani, Heart to heart: cardiospheres for myocardial regeneration, Heart Rhythm. 9 (2012) 1727–1731.
[39] S. Messaoudi, A.D. Zhang, V. Griol-Charhbili, B. Escoubet, J. Sadoshima, N. Farman, F. Jaisser, The epidermal growth factor receptor is involved in angiotensin II but not aldosterone/salt-induced cardiac remodelling, PLoS One 7 (2012) e30156.
[40] E. Messina, L. De Angelis, G. Frati, S. Morrone, S. Chimenti, F. Fiordaliso, M. Salio, M. Battaglia, M.V. Latronico, M. Coletta, E. Vivarelli, L. Frati, G. Cossu, A. Giacomello, Isolation and expansion of adult cardiac stem cells from human and murine heart, Circ. Res. 95 (2004) 911–921.
[41] N. Mohan, Y. Shen, Y. Endo, M.K. ElZarrad, Wu WJ, Trastuzumab, but not pertuzumab, dysregulates HER2 signaling to mediate inhibition of autophagy and increase in reactive oxygen species production in human cardiomyocytes, Mol. Cancer Ther. 15 (2016) 1321–1331.
[42] O. Odiete, M.F. Hill, D.B. Sawyer, Neuregulin in cardiovascular development and disease, Circ. Res. 111 (2012) 1376–1385.
[43] M.B. Olsen, G.A. Hildrestrand, K. Scheffler, L.E. Vinge, K. Alfsnes, V. Palibrk, J. Wang, C.G. Neurauter, L. Luna, J. Johansen, J.D. Ogaard, I.K. Ohm, G. Slupphaug, A. Kusnierczyk, A.E. Fiane, S.H. Brorson, L. Zhang, L. Gullestad, W.E. Louch, P.O. Iversen, I. Ostlie, A. Klungland, G. Christensen, I. Sjaastad, P. Saetrom, A. Yndestad, P. Aukrust, M. Bjoras, A.V. Finsen, NEIL3-dependent regulation of cardiac fibroblast proliferation prevents myocardial rupture, Cell Rep. 18 (2017) 82–92.
[44] C. Ozcelik, B. Erdmann, B. Pilz, N. Wettschureck, S. Britsch, N. Hubner, K.R. Chien, C. Birchmeier, A.N. Garratt, Conditional mutation of the ErbB2 (HER2) receptor in cardiomyocytes leads to dilated cardiomyopathy, Proc. Natl. Acad. Sci. U. S. A. 99 (2002) 8880–8885.
[45] D.T. Paik, M. Rai, S. Ryzhov, L.N. Sanders, O. Aisagbonhi, M.J. Funke, I. Feoktistov, A.K. Hatzopoulos, Wnt10b gain-of-function improves cardiac repair by arteriole formation and attenuation of fibrosis, Circ. Res. 117 (2015) 804–816.
[46] A. Papapetropoulos, D. Fulton, K. Mahboubi, R.G. Kalb, D.S. O'Connor, F. Li, D.C. Altieri, W.C. Sessa, Angiopoietin-1 inhibits endothelial cell apoptosis via the Akt/survivin pathway, J. Biol. Chem. 275 (2000) 9102–9105.
[47] K. Peng, X. Tian, Y. Qian, M. Skibba, C. Zou, Z. Liu, J. Wang, Z. Xu, X. Li, G. Liang, Novel EGFR inhibitors attenuate cardiac hypertrophy induced by angiotensin II, J. Cell. Mol. Med. 20 (2016) 482–494.
[48] L. Pentassuglia, P. Heim, S. Lebboukh, C. Morandi, L. Xu, M. Brink, Neuregulin-1beta promotes glucose uptake via PI3K/Akt in neonatal rat cardiomyocytes, Am. J. Physiol. Endocrinol. Metab. 310 (2016) E782–E794.
[49] J.R. Privratsky, P.J. Newman, PECAM-1: regulator of endothelial junctional integrity, Cell Tissue Res. 355 (2014) 607–619.
[50] H. Quan, S.K. Kim, S.J. Heo, J.Y. Koak, J.H. Lee, Optimization of growth inducing factors for colony forming and attachment of bone marrow-derived mesenchymal stem cells regarding bioengineering application, J. Adv. Prosthodont. 6 (2014) 379–386.
[51] G. Ren, L.H. Michael, M.L. Entman, N.G. Frangogiannis, Morphological characteristics of the microvasculature in healing myocardial infarcts, J. Histochem. Cytochem. 50 (2002) 71–79.
[52] C. Rodriguez-Antona, J. Pallares, C. Montero-Conde, L. Inglada-Perez, E. Castelblanco, I. Landa, S. Leskela, L.J. Leandro-Garcia, E. Lopez-Jimenez, R. Leton, A. Cascon, E. Lerma, M.C. Martin, M.C. Carralero, D. Mauricio, J.C. Cigudosa, X. Matias-Guiu, M. Robledo, Overexpression and activation of EGFR and VEGFR2 in medullary thyroid carcinomas is related to metastasis, Endocr. Relat. Cancer 17 (2010) 7–16.
[53] K.S. Russell, D.F. Stern, P.J. Polverini, J.R. Bender, Neuregulin activation of ErbB receptors in vascular endothelium leads to angiogenesis, Am. J. Phys. 277 (1999) H2205–11.
[54] S. Ryzhov, A.E. Goldstein, S.V. Novitskiy, M.R. Blackburn, I. Biaggioni, I. Feoktistov, Role of A2B adenosine receptors in regulation of paracrine functions of stem cell antigen 1-positive cardiac stromal cells, J. Pharmacol. Exp. Ther. 341 (2012) 764–774.
[55] S. Ryzhov, Q. Zhang, I. Biaggioni, I. Feoktistov, Adenosine A2B receptors on cardiac stem cell antigen (Sca)-1-positive stromal cells play a protective role in myocardial infarction, Am. J. Pathol. 183 (2013) 665–672.
[56] S.M. Sweeney, G. DiLullo, S.J. Slater, J. Martinez, R.V. Iozzo, J.L. Lauer-Fields, G.B. Fields, J.D.S. Antonio, Angiogenesis in collagen I requires α2β1 ligation of a GFP*GER sequence and possibly p38 MAPK activation and focal adhesion disassembly, J. Biol. Chem. 278 (2003) 30516–30524.
[57] K. Tamama, V.H. Fan, L.G. Griffith, H.C. Blair, A. Wells, Epidermal growth factor as a candidate for ex vivo expansion of bone marrow-derived mesenchymal stem cells, Stem Cells 24 (2006) 686–695.
[58] Z. Tao, B. Chen, X. Tan, Y. Zhao, L. Wang, T. Zhu, K. Cao, Z. Yang, Y.W. Kan, H. Su, Coexpression of VEGF and angiopoietin-1 promotes angiogenesis and cardiomyocyte proliferation reduces apoptosis in porcine myocardial infarction (MI) heart, Proc. Natl. Acad. Sci. U. S. A. 108 (2011) 2064–2069.
[59] H. Ushikoshi, T. Takahashi, X. Chen, N.C. Khai, M. Esaki, K. Goto, G. Takemura, R. Maruyama, S. Minatoguchi, T. Fujiwara, S. Nagano, K. Yuge, T. Kawai, Y. Murofushi, H. Fujiwara, K. Kosai, Local overexpression of HB-EGF exacerbates remodeling following myocardial infarction by activating noncardiomyocytes, Lab. Investig. 85 (2005) 862–873.
[60] M. Valente, D.S. Nascimento, A. Cumano, O.P. Pinto-do, Sca-1 + cardiac progenitor cells and heart-making: a critical synopsis, Stem Cells Dev. 23 (2014) 2263–2273.
[61] H. van Cruijsen, G. Giaccone, K. Hoekman, Epidermal growth factor receptor and angiogenesis: opportunities for combined anticancer strategies, Int. J. Cancer 117 (2005) 883–888.
[62] J.I. Virag, C.E. Murry, Myofibroblast and endothelial cell proliferation during murine myocardial infarct repair, Am. J. Pathol. 163 (2003) 2433–2440.
[63] M.C. Whelan, D.R. Senger, Collagen I initiates endothelial cell morphogenesis by inducing actin polymerization through suppression of cyclic AMP and protein kinase a, J. Biol. Chem. 278 (2003) 327–334.
[64] F. Yang, Y.H. Liu, X.P. Yang, J. Xu, A. Kapke, O.A. Carretero, Myocardial infarction and cardiac remodelling in mice, Exp. Physiol. 87 (2002) 547–555.
[65] M.R. Zile, C.F. Baicu, J.S. Ikonomidis, R.E. Stroud, P.J. Nietert, A.D. Bradshaw, R. Slater, B.M. Palmer, P. Van Buren, M. Meyer, M.M. Redfield, D.A. Bull, H.L. Granzier, M.M. LeWinter, Myocardial stiffness in patients with heart failure and a preserved ejection fraction: contributions of collagen and titin, Circulation 131 (2015) 1247–1259.